Published in final edited form as:
J Neurochem. 2006 November ; 99(4): 1207–1223. doi:10.1111/j.1471-4159.2006.04185.x.

Manipulating Kv4.2 identifies a specific component of hippocampal pyramidal neuron A-current that depends upon Kv4.2 expression

Aaron Lauver[*], **Li-Lian Yuan**[†], **Andreas Jeromin**[‡], **Brian M. Nadin**[*], **José J. Rodríguez**[§], **Heather A. Davies**[§], **Michael G. Stewart**[§], **Gang-Yi Wu**[¶], and **Paul J. Pfaffinger**[*]

[*]Department of Neuroscience, Baylor College of Medicine, Houston, Texas, USA

[†]Department of Neuroscience, University of Minnesota, Minneapolis, Minneapolis, USA

[‡]Center for Learning and Memory, University of Texas at Austin, Texas, USA

[§]Department of Biological Sciences, The Open University, Milton Keynes, UK

[¶]Department of Molecular Physiology and Biophysics, Baylor College of Medicine, Houston, Texas, USA

Abstract

The somatodendritic A-current, I_{SA}, in hippocampal CA1 pyramidal neurons regulates the processing of synaptic inputs and the amplitude of back propagating action potentials into the dendritic tree, as well as the action potential firing properties at the soma. In this study, we have used RNA interference and over-expression to show that expression of the Kv4.2 gene specifically regulates the I_{SA} component of A-current in these neurons. In dissociated hippocampal pyramidal neuron cultures, or organotypic cultured CA1 pyramidal neurons, the expression level of Kv4.2 is such that the I_{SA} channels are maintained in the population at a peak conductance of approximately 950 pS/pF. Suppression of Kv4.2 transcripts in hippocampal pyramidal neurons using an RNA interference vector suppresses I_{SA} current by 60% in 2 days, similar to the effect of expressing dominant-negative Kv4 channel constructs. Increasing the expression of Kv4.2 in these neurons increases the level of I_{SA} to 170% of the normal set point without altering the biophysical properties. Our results establish a specific role for native Kv4.2 transcripts in forming and maintaining I_{SA} current at characteristic levels in hippocampal pyramidal neurons.

Keywords

A-current; dominant–negative; hippocampal pyramidal neurons; Kv4 potassium channels; RNA interference; viral vectors

A-current is found throughout the somatodendritic compartment of pyramidal neurons and has clear functional importance in both the soma and dendrites of these cells. Dynamic regulation of the inactivated state is thought to provide an important associative signal that links patterns of electrical activity with changes in the excitability of a neuron (Schrader *et al.* 2002; Watanabe *et al.* 2002; Frick *et al.* 2004). In hippocampal CA1 pyramidal neurons, A-currents regulate the processing of synaptic inputs in the dendritic tree, the amplitude of

Address correspondence and reprint requests to Paul J. Pfaffinger, Department of Neuroscience, Baylor College of Medicine, One Baylor Plaza, S630, Houston, TX 77030 USA. paulp@bcm.tmc.edu.

back propagating action potentials into the dendritic tree, as well as the neuronal action potential firing properties at the soma (Hoffman *et al.* 1997; Ramakers and Storm 2002; Cai *et al.* 2004; Kim *et al.* 2005). Dynamic regulation of A-current levels produces excitability changes that can be seen at the level of a whole neuron, or within a small well-defined region of the dendritic tree (Ramakers and Storm 2002; Johnston *et al.* 2003; Cai *et al.* 2004; Frick *et al.* 2004; Kim *et al.* 2005).

A fundamental problem in neuroscience is the identification of native ion channels that are formed from specific genes in order to understand how regulation of these genes translates into changes in cellular electrophysiological properties. For our studies, we are interested in the expression and regulation of the I_{SA} component of A-current (Jerng *et al.* 2004b). I_{SA} is the classic, 'subthreshold' A-type current and is often referred to only as the A-current; however, biophysical studies in numerous cell types, including our studies here, clearly show that multiple A-type currents are found in individual neurons, and that the I_{SA} current is a specific component of this overall A-current (Surmeier *et al.* 1989; Wu and Barish 1992; Mu *et al.* 1999; Chen and Johnston 2004).

Several previous studies have attempted to determine the underlying gene products responsible for forming A-currents in hippocampal pyramidal neurons (Ramakers and Storm 2002; Cai *et al.* 2004; Kim *et al.* 2005). These studies have shown that dominant -negative Kv4 constructs, as well as heteropodotoxins, which appear specific to Kv4 channels, suppress A-currents in these neurons. However, these previous studies, while offering important insights into the physiological and functional roles of Kv4 channels in pyramidal neurons, did not identify a specific gene product responsible for forming a specific component of A-current because of intrinsic limitations in the methods used in these studies. In this work, in order to overcome the limitations present in these previous studies on hippocampal pyramidal neurons, we have taken a novel approach to test if a specific gene, Kv4.2 (KCND2), is responsible for forming the I_{SA} component of A-current in hippocampal pyramidal neurons. First, we have carefully separated the different A-current components in these neurons to determine if there is a specific effect of manipulating Kv4.2 only on the I_{SA} component of the A-current. Previous studies in the heart have shown that Kv4 subunits are only responsible for forming one specific component of the A-current called $I_{to,f}$ (Barry *et al.* 1998; Wickenden *et al.* 1999; Guo *et al.* 2005). In hippocampal neurons, previous dominant-negative and toxin studies have not clearly separated out the different current components forming A-current in these neurons to determine which components are selectively formed from Kv4 channels (Ramakers and Storm 2002; Cai *et al.* 2004; Kim *et al.* 2005). Second, in order to directly address the molecular link between a specific channel gene and a native ion channel type, we have turned to RNA interference (RNAi) technology as a means to acutely suppress a specific channel gene to probe the importance of that gene in forming the native channel (Brummelkamp *et al.* 2002; Couzin 2002). By down-regulating transcription of the Kv4.2 channel gene using RNA interference, and up-regulating the same transcript using over-expression vectors, we tested if changes in the expression of Kv4.2 are linked to changes in I_{SA} current amplitude or biophysical properties in hippocampal pyramidal neurons. Previous studies using dominant negatives or toxins could only implicate Kv4 family members in the formation of A-type currents, but not a specific gene product. Our studies, presented here, provide strong direct experimental evidence for a specific role of the Kv4.2 gene in the formation of the I_{SA} current in hippocampal pyramidal neurons, as well as a role for Kv4.2 transcript levels in regulating the amplitude of the specific I_{SA} current component.

Materials and methods

Cloning and molecular biology

Our RNA interference vector, pSuperRed, was constructed by moving the shRNA expression cassette from the origin H1 variant of pSuper (Brummelkamp *et al.* 2002), into the pDsRed2-C1 vector (BD Biosciences Clontech, Palo Alto, CA, USA) which provides Kan/Neo selection along with CMV promoter diving expression of DsRed2 fluorescent proteins. We first removed *Bgl*II and *Hind*III sites from the pDsRed2-C1 vector polylinker to free these sites up for cloning of double-stranded oligos into the shRNA expression cassette. A 310-bp fragment from modified pDsRed2-C1 was removed by a full digestion with *Dra*III and a partial digestion with *Bsp*H1. An H1 promoter cassette for expression of shRNAs was prepared by cutting the H1 variant of pSuper with *Dra*III and *Afl*III. This fragment was cloned into the modified pDsRed2-C1 to create pSuperRed, see Fig. 4. Interfering RNAs were cloned into the *Bgl*II and *Hind*III sites that follow the H1 promoter as shRNAs. Kv4.2 was screened for likely RNAi target sequences using the criteria of Brummelkamp *et al.* (2002). Two target sequences were identified in the rat Kv4.2 sequence that corresponded to a AA(N19)TTconsensus with 30–70% GC content. The most effective sequence, used to make pSuperRed-Kv4.2i, is AA**AGGACTCAGGACGCTCTAA**TT which targets the CDS of rKv4.2 at residues 106–128 (shown in bold). The shRNA insert for pSuperRed-Kv4.2i was made by cloning the following sequence: CCC**AGGACTCAGGACGCTCTAA** ttcaagaga**TTAGAGCGTCCTGAGTCCT**TTTTTGGAAA into *Bgl*II + *Hind*III cut pSuperRed by ligation of double-strand oligonucleotides with GATC and AGCT sticky ends. Our dominant-negative Kv4 construct, Kv4DN-enhanced green fluorescent protein (EGFP), was a kind gift of David Johns (Johns Hopkins, Baltimore, MD, USA), and has been described and characterized previously as GFP-Kv4.2ST (Johns *et al.* 1997). This construct acts as a dominant negative because EGFP is cloned into the Pore region of Kv4.2, thus creating a truncated dominant-negative subunit, that retains the T1 assembly domain, but lacks the required pore-forming sequence to create functional channels. Kv4DN-EGFP was cloned into pSinRep5 (Invitrogen, Carlsbad, CA, USA) to make pSindbis-Kv4DN-EGFP. A dual subgenomic vector co-expressing EGFP with Kv4.2 was also made (Green-Sindbis-Kv4.2). Recombinant Sindbis viruses were generated as described previously (Jeromin *et al.* 2003). Briefly, RNA was transcribed *in vitro* from the pSindbis vectors and the DH-26S helper plasmid using the Megascript kit (Ambion, Austin, TX, USA). Sindbis and DH-26S RNAs were co-electroporated into BHK cells (ATCC, Manassas, VA, USA) using either an Invitrogen electroporator or the Bio-Rad II gene pulser (Bio-Rad Laboratories, Hercules, CA, USA). The use of the DH-26S helper ensured the preferential infection of neurons in slices. Supernatants containing the recombinant virus were harvested 48–72 h after electroporation, and the titer of the harvested viruses was typically in the range of 10^8–10^9/mL.

COS7 cell culture and transfection

COS7 cells (ATCC) were grown in Dulbecco's modified Eagle's medium plus 10% fetal bovine serum (HyClone, Logan, UT, USA) and 1% penicillin/streptomycin (Invitrogen). Cells were plated at a density of 150 000 cells per 35-mm dish, grown overnight and transfected the next day with Fugene6 (Roche Molecular Biochemicals, Indianapolis, IN, USA) following the manufacturer's protocols. To test pSuperRed constructs, cells were co-transfected with the pSuperRed-RNAi vector and a pCMV-target expressing vector. After 48 h, the cells were harvested and the expression level for the target protein was assayed by western blotting.

Dissociated hippocampal culture and transfection

All animal procedures were conducted in accordance with the policies of AALAC and Baylor College of Medicine IACUC. Methods for dissociated culture of CA1-CA3 neurons from 0- to 3-day-old Sprague–Dawley rats were adapted from Malgaroli and Tsien (1992). Glass coverslips (12 mm round) were placed in 24-well plates and coated with a 1/20–1/50 solution of Matrigel (BD Biosciences Clontech) and growth medium immediately prior to the neuron dissociation protocol. Post-natal day 1-2 rat pups (Sprague–Dawley; Harlan Inc., Indianapolis, IN, USA) were killed by decapitation and the brains were immediately placed in divalent-free Hank's salt solution (Sigma, St Louis, MO, USA) plus 20% fetal calf serum (HyClone). Hippocampi were isolated from the rest of the brain and, in subsequent steps, particular attention was paid to removal of the entorhinal cortex and subiculum, as well as all visible vasculature. The hippocampi were then placed in fresh Hank's salt solution + 20% fetal calf serum medium and crudely dissociated using a scalpel. Hippocampi were digested at 37 °C for 10 min in a digestion solution containing 10 mg/mL trypsin (Sigma), washed, and then mechanically triturated in dissociation solution containing Hank's salt solution plus $MgSO_4$ using siliconized pipettes. After dissociation, cells were spun at 1000 *g* for 10 min, re-suspended in growth medium, and plated at a density of 2000–5000 cells per well. One litre of basic culture medium consisted of phenol-free minimal essential medium (MEM; Invitrogen) supplemented with 5 g glucose (Sigma), 200 mg $NaHCO_3$ (Sigma), and 100 mg Transferrin (Calbiochem, La Jolla, CA, USA). Growth medium consisted of basic culture medium plus 5% fetal bovine serum (HyClone), 2% B-27 supplement (Invitrogen), 500 nM L-glutamine (Sigma), and 2–4 μM cytosine-D-arabinofuranoside (Sigma). For some experiments, 0.25 g/L insulin (Sigma) was also included in the culture media. Cultures were maintained at 37 °C in a 5% CO_2-humidified incubator for 7–14 days in growth medium prior to transfection. Transfection was performed using either Lipofectamine 2000 (Invitrogen) or Ca-phosphate precipitation. For Lipofectamine 2000, growth medium was removed and cultures were washed once with serum-free medium. For each well, a 100-μL mixture of Lipofectamine 2000 (2 μL), DNA (1 μL), and serum-free medium (97 μL) was added directly to the coverslip in a drop-wise manner. Subsequently, 300 lL of growth medium was added to each well and cultures were incubated for 24–48 h before analysis. For Ca-phosphate transfections, neuronal cultures were washed twice with fresh, serum-free medium (MEM + 5 g/L glucose) after saving the original media. A total of 2 μg DNA was mixed with 2 μL 2 M $CaCl_2$ and distilled water in a volume of 15 μL, and then an equal volume of 2 × HEPES-buffered saline (BD Biosciences Clontech) was added to a total volume of 30 lL. After 5 min at 22 °C, the mixed solution was added drop-wise to each coverslip, and the cells were returned to the incubator (37 °C) for 30–45min. To minimize cytotoxicity and optimize transfection efficiency, the precipitate was closely monitored; when a layer of precipitate became obvious, cells were washed three times with MEM and returned to the saved original medium.

Organotypic slice culture and Sindbis viral infection

Organotypic slices were prepared and cultured according to the interface technique as originally described by Stoppini *et al.* (1991) and Jeromin *et al.* (2003). Infection of neurons with Sindbis virus was accomplished by focal injection in CA1 pyramidal neurons in organotypic slices or application to primary cultures of hippocampal neurons (Jeromin *et al.* 2003).

Electrophysiology and light microscopy

Neurons were visualized using upright microscopes equipped with IR-DIC and epifluorescence (either an Olympus BX51 upright microscope with a 60 × water immersion objective or a Zeiss Axioskop with a 40 × water-immersion objective). Voltage-clamp protocols were conducted in whole-cell configuration using Axo-patch 200b amplifiers.

Pulse generation and data acquisition were controlled with either custom software written for the Igor Pro analysis environment (Yuan *et al.* 2002), or pClamp7–9 software. Whole-cell capacitance and series resistances were compensated to more than 80%, and series resistances were less than two times the tip resistance. Leakage and capacitive currents were digitally subtracted online. Current inactivation kinetics was determined by single exponential curve fitting. Significance ($p < 0.05$) was determined by two-sample t-tests. Error bars represent SE. Voltage-clamp protocols to isolate current components are described in the text.

Neurons were recorded in a perfusion chamber at 22 °C for all experiments. To avoid variations in native I_{SA} density, and to reduce the complexity of the molecular identity of native I_{SA} among different cell types, we chose to restrict our studies to a subset of transfected pyramidal-shaped neurons with a major apical dendrite, some basal dendrites, and a relatively small soma with a whole-cell capacitance around 20 pF. Bath solution was continuously bubbled with a 95%/5% mixture of O_2/CO_2 and consisted of, in mM:NaCl 125, KCl 2.5, $NaHCO_3$ 25, $CaCl_2$ 2, $MgCl_2$ 2, dextrose 10. Tetrodotoxin (Tocris, Ellisville, MO, USA) was added to the bath solution prior to experiments at 1–2-μM concentrations. Heteropodatoxin-3 (HpTx3; NPS Pharmaceuticals, Salt Lake City, UT, USA) was dissolved in water and added to the external solution with 0.1% bovine serum albumin. Capillaries (1.5 mm) were pulled to resistances of between 3 and 6 MΩ and were filled with internal solution consisting of, in mM: Kgluconote 120, KCl 20, NaCl 5, HEPES 10, Mg-ATP 4, Tris-GTP 3, phosphocreatine 14. In some experiments, to further isolate Kv currents, 2 mM $MnCl_2$ was substituted for $CaCl_2$ in the bath to block Ca^{2+} currents, and Ca^{2+}-activated K^+ currents. Activation and inactivation data analyzed as both fits to averaged data (presented in the figures), and averaged data for the fits to individual experiments, used to determine mean and standard error. Numbers (n) of 7–16 were used in these experiments. There were no significant differences in the average activation or inactivation gating properties of I_{SA}, I_{AD} or I_{SS} with knockdown or over-expression of Kv4.2.

Current isolation and quantification protocols

For isolation of I_{SA}, we subtracted recordings performed at test potentials from −70 to +50 mV, obtained by holding, or pre-pulsing from 200 ms to 1 s, at −30 to −40 mV from matched recordings obtained by pre-pulsing or holding at more negative potentials, typically −80 to −100 mV. The subtraction selectively removes the I_{AD} and I_{SS} components from the recording. Note that this protocol produces a small subtraction artifact in the pre-pulse as a result of the partial activation of I_{SS} currents at −30 mV. This artifact causes the pre-pulse baseline current to jump around in Fig. 5(c) and Fig. 6(c). For I_{AD}, we subtracted recordings performed at test potentials from −40 to +90 mV obtained by pre-pulsing for 500 ms to 1 s, at +50 mV, then stepping to −30 mV for 10 ms, from recordings obtained by holding or pre-pulsing for 500 ms to 1 s at −30 mV. This procedure subtracts I_{SS} from combined I_{AD} and I_{SS} recordings. The brief step to −30 mV was carried out to obtain more accurate subtractions by closing I_{SS} channels before the subtraction. For I_{SS}, we held at +50 ms for 500 to 1 s to inactivate all A-type channels, stepped to −30 mV for 10 ms to close I_{SS} channels, then applied a series of activation pulses to record an isolated I_{SS} current. To quantify the magnitude of three current components in the same recordings, we constructed inactivation curves as shown in Fig. 1(b), then fit these curves for the two Boltzmann components and the residual non-inactivating component. The I_{SA} amplitude was obtained by the amplitude of the most negative Boltzmann component, the I_{AD} amplitude was obtained by the amplitude of the less negative component, and the I_{SS} component was obtained by the residual component. We also separately verified that the amplitudes of these current components measured from the inactivation curve closely matched the amplitudes of the isolated currents recorded as described above.

Western blotting and luminance densitometry

Whole cell lysates were separated by sodium dodecyl sulfate – polyacrylamide gel electrophoresis and transferred to Immobilon filters (Millipore Corporation, Bedford, MA, USA). Every gel contained both a control and experimental condition transfected in triplicate, and was probed either simultaneously or sequentially for the protein of interest. Glyceraldehyde 3-phosphate dehydrogenase (GAPDH) levels were also probed by western blotting to serve as an internal control. The following primary antibodies were used: anti-kv4.2 (rabbit, AB no. 5362; Chemicon, Temecula, CA, USA), anti-Kv4.3 (goat, n15; Santa Cruz Biotechnology, Santa Cruz, CA, USA), anti-Kv1.4 (rabbit, Ab5926; Chemicon), anti-KChIP3 (rab-bit, FL-214; Santa Cruz Biotechnology), and anti-GAPDH (mouse, clone 6c5; Advanced Immunochemicals, Long Beach, CA, USA). Horseraddish peroxidase-conjugated secondary antibodies (Pierce, Rockford, IL, USA) were used for secondary antibody detection on Kodak MR Film. Films were scanned into a computer and luminance densitometry was performed using Optiquant software (Perkin Elmer, Wellesley, MA, USA).

Immunoelectron microscopy

Organotypic hippocampal slices were fixed by immersion with 3.75% acrolein in a solution of 2% paraformaldehyde and 0.1 M phosphate buffer (PB), pH 7.4, for 1 h. The slices were then post-fixed for 1–2 h in 2% paraformaldehyde. To remove the excess of reactive aldehydes, sections were treated with 1% sodium borohydride in 0.1 M PB for 30 min. Sections were then rinsed with 0.1 M PB followed by 0.1 M Tris-buffered saline, pH 7.6. Hippocampal slices were processed for immunoperoxidase and immunogold-silver labeling of Kv4DN-EGFP prior to plastic embedding using an affinity-purified rabbit polyclonal antibody directed against highly purified recombinant EGFP made in *Escherichia coli* (Abcam Ltd, Cambridge, UK). The selectivity of this antibody has been established by western blotting, immunoprecipitation and immunofluorescence experiments (Jasinska *et al.* 1999; McCabe and Berthiaume 1999). In addition, no labeling was seen in uninfected neurons or when the antibody was omitted from the reaction procedure. For this experiment, the slices were first incubated for 30 min in 0.5% bovine serum albumin in Tris-buffered saline to minimize non-specific labeling. The slices then were incubated for 48 h at 4 °C in 0.1% bovine serum albumin in Tris-buffered saline containing rabbit polyclonal antiserum for EGFP (1: 500 dilution for immunoperoxidase, 1: 100 dilution for immunogold). Subsequently, the EGFP antibody was detected by using the pre-embedding immunoperoxidase or immunogold-silver methods. Immunolabeled hippocampal slices were rinsed in 0.1 M PB pH 7.4, and then post-fixed for 1 h in 2% osmium tetroxide in PB. They were subsequently dehydrated through a graded series of ethanols and propylene oxide prior to embedding in Epon 812 (Shell Chemicals, London, UK) between sheets of Aclar plastic (Honeywell, Morristown, NJ, USA). Ultrathin sections were cut with a diamond knife (Diatome, Fort Washington, PA, USA), and collected on copper mesh grids. The sections on grids were counterstained with uranyl acetate and lead citrate, and examined with a JEOL 1010 electron microscope (Reynolds 1963).

Results

Voltage-clamp separation of currents in native neurons

We first developed biophysical protocols to separate the major components of inactivating current in our hippocampal neuronal cultures to determine if we could isolate a clear I_{SA} component from other voltage-gated potassium currents. Hippocampal neuronal cultures from post-natal day 2 rats were prepared and cultured for 9–14 days. Pyramidal-shaped neurons with capacitances around 20–25 pF were selected for our whole-cell voltage-clamp recordings. A steady-state inactivation protocol was applied by holding neurons at −80 mV

and then pre-pulsing to potentials between −100 mV and +40 mV, before applying a test pulse to +50 mV. As can be seen in the recordings from a representative cell, a pre-pulse potential to −100 mV reveals a large component of inactivating current that is progressively lost at more positive pre-pulse potentials (Fig. 1a). Interestingly, at a middle potential range in the −40 to −30 mV range, the inactivation curve flattens out before becoming steeper again around −10 mV, and then flattens out again with a substantial component of non-inactivating current. When peak current is plotted versus potential, two clear components of inactivating current can be seen (Fig. 1b). Double Boltzman fits show that the more negative inactivating component has an inactivation midpoint of −70.1 ± 2.2 mV, as expected for I_{SA}. The more positive inactivating component has a midpoint of −11.4 ± 2.3 mV, and seems to correspond well to a '$_D$-type' inactivating channel described in cultured hippocampal pyramidal neurons and in patch recordings from rat hippocampal dendrites (Mu *et al.* 1999; Chen and Johnston 2004). We will refer to this as the I_{AD} current. Finally, the non-inactivating voltage-gated *K* current, likely composed of M-channels and delayed rectifier channels, will be referred to as the sustained current, I_{SS} (Gu *et al.* 2005; Misonou *et al.* 2005). I_{SA} can easily be separated from the other components by using a difference current measurement between traces recorded with pre-pulses to −100 mV versus −30 mV. As can be seen in Fig. 1(c), subtraction of the −30 mV traces from the −100 mV traces reveals the rapidly inactivating I_{SA} current. Using this isolation protocol, we characterized the peak activation properties of I_{SA} in our neurons and plotted the peak conductance probability versus potential in Fig. 2(a). The measured midpoint for peak activation of this channel is −22.1 ± 2.9 mV. If neurons are held at more positive potentials, we can also characterize the activation properties of I_{AD} and I_{SS}. To isolate I_{AD}, a difference current method was applied. Voltage steps from a holding potential of −30 mV activate both I_{AD} and I_{SS}. Applying a pre-pulse to +40 mV inactivates I_{AD}, allowing us to selectively record I_{SS}. Because this pre-pulse potential is large enough to activate I_{SS}, we applied a brief pulse to −30 mV to shut the I_{SS} channels before applying the test pulses. The I_{SS} current activation curve obtained in this manner has a half activation point of 2.8 ± 2.7 mV (Fig. 2c). Subtraction of the I_{SS} current from the current recorded from a holding potential of −30 mV reveals the more slowly inactivating I_{AD} current with an inactivation time constant of 117 ± 18 ms at +50 mV (Fig. 2b). The activation curve obtained from this subtraction suggests a half activation point of +28.9 ± 3.3 mV for I_{AD}.

Sensitivity of the I_{SA} current to HpTx3

We next sought to determine if the current we have identified as I_{SA} is sensitive to the toxin heteropodatoxin-3, HpTx3. In heterologous expression systems, heteropodatoxins have been shown to selectively suppress the Kv4 class of potassium channel (Sanguinetti *et al.* 1997; Bernard *et al.* 2000; Zarayskiy *et al.* 2005). Previous studies on CA1 pyramidal neurons in acute slices have shown that at least part of the A-current in these neurons is sensitive to heteropodatoxin (Ramakers and Storm 2002). The toxins appear to act by modulating the gating properties of Kv4 channels, producing a strong suppression of Kv4 channel currents at negative potentials that is relieved at more positive potentials (Sanguinetti *et al.* 1997; Zarayskiy *et al.* 2005). Whole-cell voltage-clamp recordings were obtained on hippocampal pyramidal neurons in culture and sensitivity of currents was tested by application of 100 n_M HpTx3. As can be seen in Fig. 3(a), 100 n_M HpTx3 produces a selective reduction in the fast inactivating I_{SA} component of current with no effects on the slower inactivating I_{AD} or sustained I_{SS} components. We next compared the ability of HpTx3 to suppress I_{SA} current at different test potentials (Fig. 3b). The results show a clear voltage dependence to HpTx3 suppression of I_{SA}, with a near 100% block at −40 mV reduced to a 40% block at 0 mV, similar to the results previously described on Kv4.2 in heterologous systems (Sanguinetti *et al.* 1997; Zarayskiy *et al.* 2005).

Construction of RNAi vectors to suppress Kv4.2

Previous studies have suggested that the I_{SA} current in a variety of neurons is likely made from Kv4 family proteins (Baldwin *et al.* 1991; Sheng *et al.* 1992; Serodio *et al.* 1996; Jan and January 1997; Song *et al.* 1998; Tkatch *et al.* 2000; Jerng *et al.* 2004b). In situ hybridization and immunostaining have shown that Kv4.2 is expressed in hippocampal pyramidal neurons, making it a logical candidate gene for formation of I_{SA} in our neurons (Serodio *et al.* 1996; Rhodes *et al.* 2004). To directly test this hypothesis, we constructed an RNA interference vector that allows us to knock down specific mRNAs, while marking transfected neurons with a red fluorescent protein, by cloning the H1 promoter region from pSuper into pDsRed2-C1 (Clontech) to make pSuperRed, see Fig. 4(a and b). RNAi targets on Kv4.2 were identified and screened by blast searching to confirm that they are uniquely present on Kv4.2. To express RNAi, shRNAs containing the RNAi inserts were designed as 64-base complementary DNA oligonucleotide pairs (Sigma Genosys, Houston, TX, USA) with 5′ overhangs matching the *Bgl*II and *Hind*III restriction sites that follow the H1 promoter on pSuperRed. Constructs were tested by co-transfection of pSuperRed with pCMV-Kv4.2 into COS7 cells and western blotting. An effective RNAi sequence was identified that corresponds to a 19-bp sequence 108–126 bases downstream of the rat Kv4.2 start codon to make pSuperRed-Kv4.2i. Following co-transfection of COS7 cells with pCMV-Kv4.2 plus pSuperRed or pSuperRed-Kv4.2i, the expression of Kv4.2 protein was dramatically reduced only in the presence of pSuperRed-Kv4.2i (Fig. 4c). We confirmed the specificity of pSuperRed-Kv4.2i by testing if expression of other proteins that might contribute to forming transient potassium currents in hippocampal pyramidal neurons were affected by pSuperRed-Kv4.2i. As can be seen in Fig. 4(d), following co-transfection of pSuperRed-Kv4.2i with a series of potential target constructs in COS7 cells, pSuperRed-Kv4.2i specifically knocks down the expression of Kv4.2 by over 80%, but has no effect on the expression of Kv4.3, Kv1.4, or KChIP3. In addition, the endogenous expression of GAPDH is not affected by pSuperRed-Kv4.2i. As expected, the control vector pSuperRed has no effect on expression of any of these proteins, showing that the selective knockdown of Kv4.2 by pSuperRed-Kv4.2i is specifically produced by the inserted RNAi sequence.

Sensitivity of voltage-gated potassium currents to Kv4.2 RNAi expressed in neurons

Our recordings show that an I_{SA} current that is sensitive to HpTx3 is present in whole-cell recordings from cultured rat hippocampal pyramidal neurons. Therefore we next sought to test if Kv4.2 is necessary for expression of I_{SA} in these neurons by suppression of Kv4.2 using RNA interference. Hippocampal neurons in culture were transfected with pSuperRed or pSuperRed-Kv4.2i and examined 48 h after transfection. Approximately 1–5% of the neurons in these cultures were transfected under these conditions. Red fluorescent neurons with pyramidal shapes were selected for voltage-clamp recordings, see Fig. 4(b). Current components were isolated using the differential inactivation properties described previously. The properties and the amplitudes of these current components were compared with and without the expression of Kv4.2 RNAi. A consistent finding in these studies was that the isolated I_{SA} current component is reduced in neurons transfected with pSuperRed-Kv4.2i, see Fig. 5(a). Separation of all three current components and analysis of the average amplitude data (Fig. 5b), shows the effects of Kv4.2 RNAi are specific to the reduction of I_{SA} current amplitude by an average of approximately 60%. The measured I_{SA} current in neurons expressing pSuperRed-Kv4.2i is significantly different from both untransfected neurons or neurons expressing pSuperRed alone. There is no significant difference in I_{SA} current amplitude produced by the control pSuperRed vector. The data also show that there are no significant differences in I_{AD} or I_{SS} current amplitudes between control neurons, pSuperRed transfected neurons or neurons transfected with pSuperRed-Kv4.2i.

The primary effects of Kv4.2 RNAi on I_{SA} are only on the amplitude of the I_{SA} current. No significant differences were observed in the activation or inactivation properties of any of the current components following transfection with pSuperRed-Kv4.2i. Scaled I_{SA} current traces in response to a pulse to +40 mV show that the residual I_{SA} current after Kv4.2 RNAi is kinetically similar to the overall I_{SA} current, see Fig. 5(c), as are the steady-state activation and inactivation curves (Fig. 5d). The inactivation time courses for the normal I_{SA} current and residual I_{SA} compared across a range of voltages in the two conditions are not significantly different (Fig. 5e).

Representative currents and summary data for Kv4.2 expressed in neurons

Expression of Kv4.2 RNAi in hippocampal pyramidal neurons shows that I_{SA} current is very sensitive to the suppression of Kv4.2 expression. Next, we wished to test if increases in the expression of Kv4.2 can specifically increase the amplitude of I_{SA} to determine if Kv4.2 message levels control the amplitude of I_{SA} current. Neurons were co-transfected with pSuperRed along with pCMV-Kv4.2 and compared 48 h after transfection with neurons transfected with pSuperRed alone. Red fluorescent neurons with a clear pyramidal shape were selected for voltage-clamp studies to determine if the increase in Kv4.2 expression specifically modulates a single component of voltage-gated potassium current. The current components were isolated as described previously and compared. Increasing the expression of Kv4.2 had a clear specific effect to increase the amplitude of the I_{SA} component with no significant changes in the I_{AD} or I_{SS} currents (Figs 6a and b). We further characterized the biophysical properties of the isolated I_{SA} currents under the normal and over-expressing conditions. The results were strikingly similar in the two cases. When scaled to the same size, the I_{SA} currents in neurons over-expressing Kv4.2 have a similar shape to those from control neurons (Fig. 6c). In addition, the time constants and voltage dependence for activation and inactivation are similar between control and Kv4.2 over-expressing neurons, see Fig. 6(d and e). These results strongly support our hypothesis that Kv4.2 message levels control the amplitude of the I_{SA} current in hippocampal pyramidal neurons.

Recovery from inactivation for neurons with and without RNAi or Kv4.2 expression

We next examined the rate of recovery from inactivation for transient potassium channels with and without changes in Kv4.2 transcription (Fig. 7a). Recovery from inactivation was characterized using a standard two-pulse protocol, where the time of the interpulse potential at −90 mV was varied. The amplitude of the current in the second pulse was compared with the first pulse and plotted versus the time at −90 mV. Control neurons show two clear components of recovery from inactivation at −90 mV, one with a time constant of 34.1 ± 2.4 ms and a second slower recovering component with a time constant of 542 ± 123 ms. Recovery traces were recorded and compared between control neurons expressing pSuperRed with those expressing either pSuperRed-Kv4.2i or co-expressing pCMV-Kv4.2 with pSuperRed. The plots show that the time constants of the two components in the different conditions were not significantly different, but the amplitudes are significantly changed (Fig. 7b). In the presence of pSuperRed-Kv4.2i, the more rapidly recovering component is smaller in amplitude compared with the slower component, and the opposite is true with the increase in expression of Kv4.2 using pCMV-Kv4.2 (%Fast amp: pSuperRed, 74 ± 3%; pSuperRed-Kv4.2i, 53 ± 5%; pCMV-Kv4.2, 87 ± 2%). These results suggest that the faster component is dependent upon the Kv4.2 expression level for Kv4.2. To confirm this result and link the faster component to I_{SA} and the slower component to I_{AD}, we compared the amplitudes of the isolated current components in these neurons to the amplitudes of the fast and slow recovery components. In Fig. 7(c), we plot the summary data comparing the fraction of total transient current that is I_{SA} with the fraction of the total recovery that occurs with the fast kinetic for neurons expressing pCMV-Kv4.2, pSuperRed, and pSuperRed-Kv4.2i. The identity line is drawn to show the expected result if the two

components are identical. The results closely match the predicted trend line, supporting an identity of the fast component matching recovery of the I_{SA} channels and the slower component as the I_{AD} recovery that is not sensitive to Kv4.2 expression levels.

Comparison of Kv4 dominant negative to suppression of Kv4.2 with RNAi

We next sought to compare the effects of dominant-negative Kv4 constructs, that suppress the functional expression of all Kv4 channels, to the specific effects of suppressing Kv4.2 with RNA interference. A GFP-tagged dominant negative Kv4 subunit (Kv4DN-EGFP) was expressed in our cultured hippocampal pyramidal neurons using a CMV promoter vector (pCMV-Kv4DN-EGFP). Currents in neurons expressing pCMV-Kv4DN-EGFP were compared with neurons expressing pCMV-EGFP. Similar to our results with Kv4.2 RNAi, and in agreement with results from Kv4 dominant-negative constructs expressed in other systems, we see a selective reduction in I_{SA} current amplitude following expression of Kv4DN-EGFP compared with control (Cai *et al.* 2004; Kim *et al.* 2005). The magnitude of the suppression of I_{SA} with pCMV-Kv4DN-EGFP was compared with the suppression seen with pSuperRed-Kv4.2i (Fig. 8a). Both constructs produced an approximate 60% suppression of I_{SA} by 48 h, significantly different from control. We do not detect a significant difference in the magnitude of the current that is suppressed when comparing between Kv4DN-EGFP and Kv4.2 RNAi.

To further confirm that the dominant-negative Kv4 subunits are suppressing the same component of current as Kv4.2 RNAi, we characterized the effects of Kv4DN-EGFP on the recovery from inactivation. Neurons were transfected with pCMV-EGFP or pCMV-Kv4DN-EGFP and recovery from inactivation characterized using a two-pulse protocol as described above, see Fig. 8(b). The magnitude of the transient current in the second pulse relative to the first pulse was plotted versus the recovery time in Fig. 8(c). As described previously, the recovery follows a double exponential time course. There was no significant difference in the time constants for recovery when comparing control with Kv4DN-EGFP; however, the amplitude of the two components was significantly changed, see Fig. 8(d). The relative amplitude of the fast component was reduced compared with the slower component following expression of Kv4DN-EGFP. These results are again in good agreement with our studies using Kv4.2 RNAi, where a selective change in the recovery of the fast component was linked to the magnitude of change in the I_{SA} current, see Fig. 7(d). We therefore conclude that Kv4.2 RNA interference and Kv4DN-EGFP both selectively suppress the I_{SA} current in cultured hippocampal pyramidal neurons to a similar extent.

Comparing I_{SA} modulation in CA1 neurons in organotypic slice cultures to dissociated hippocampal pyramidal neurons

Our studies show that the amplitude of the I_{SA} current in hippocampal pyramidal neurons in culture is dramatically modulated by manipulations that increase or decrease the levels of Kv4.2 transcripts. Next, we wanted to extend these results to a specific neuronal population, CA1 pyramidal neurons. To accomplish this, we switched to organotypic slice cultures of hippocampus and the use of Sindbis viral vectors to modulate I_{SA} currents (Jeromin *et al.* 2003). We developed two different Sindbis vectors to modulate I_{SA} currents: (i) Sindbis-Kv4DN-EGFP which expresses the same EGFP tagged dominant negative Kv4 constructs; and (ii) a dual SGP promoter Sindbis vector that expresses EGFP from one promoter and Kv4.2 from another promoter (Green-Sindbis-Kv4.2). These two constructs closely mimic the CMV promoter constructs we used in dissociated culture and should allow us to compare the results from these two systems.

Neurons were infected in organotypic culture by focal injection of viral stocks into the CA1 pyramidal neuron layer of the cultured slice. Within 24 h, green fluorescent neurons could

be detected that remained healthy by visual inspection and basic physiological parameters for the duration of the experiments (data not shown, see also Jeromin *et al.* 2003). Visually these vectors produce different patterns of green fluorescence when infected in neurons. When infected with Green-Sindbis-Kv4.2, the entire body and processes of the neuron fill completely with green fluorescence, Fig. 9(a). In contrast, the Sindbis-Kv4DN-EGFP construct shows a punctuate distribution of green fluorescence that is restricted to the somatodendritic compartment (Fig. 9b).

Previous studies in the heart have suggested that long-term exposure to dominant negative Kv4 constructs can produce structural changes in the heart that are likely unrelated to the specific effects of these constructs on $I_{to,f}$ (Wickenden *et al.* 1999; Guo *et al.* 2005). To rule out obvious cytological effects in neurons during short-term exposure to these dominant negative viral constructs, and to further examine the subcellular basis for the observed punctate protein distribution, we performed immuno-electron microscopy on CA1 pyramidal neurons expressing Sindbis-Kv4DN-EGFP, stained with anti-EGFP antibodies. Following labeling with this specific antibody, electron microscopy revealed that only a subset of neurons in fields infected with our viral vector constructs showed the specific immuno-EM signals. Immunoperoxidase staining (open arrows) of the soma of infected neurons shows extensive labeling of internal membranes of the endoplasmic reticulum (ER) and Golgi stacks of neurons expressing Kv4DN-EGFP (Fig. 9c). No labeling is seen in uninfected neurons, or in terminals from uninfected neuron terminals (UT) that abut the soma of the infected neuron. Analysis of the structure of infected neurons revealed that there were no obvious cytological differences between labeled and unlabeled neurons in the same slices. Our analysis of the basis for the punctate distribution of this protein in dendrites (Fig. 9d) suggests that most of the puncta (open arrows) are associated with collections of protein in ER and multivessicular bodies and not with a specific incorporation of these constructs into asymmetric synapses (filled arrows). To quantitate the subcellular distribution of protein within the neuron, immunogold detection was performed (Fig. 9e). Of the 78 gold particles analyzed in the dendrites, only 12 (15%) were associated with surface membranes. The remaining particles were in cytosolic compartments often associated with ER or transport vesicles. In CHO cells, Kv4DN-EGFP also shows a concentration of labeling of intracellular membranes, in agreement with our results here (Johns *et al.* 1997). We therefore conclude that short-term use of such dominant negative viral constructs does not produce disruption of normal cytology and produces proteins that are largely found in internal membranes of the somatodendritic compartment.

Next, CA1 pyramidal neurons infected with Sindbis vectors were recorded by whole-cell patch clamp to compare the functional effects of these manipulations with our studies on dissociated hippocampal neurons in culture. We first compared the resting potential of control and infected neurons and found that there were no significant differences (uninfected: $V_m = -61 \pm 1.3$ mV, $n = 13$; infected: $V_m = -61.6 \pm 1.2$ mV, $n = 15$), further supporting electron microscopy picture that these neurons are essentially healthy 2 days following infection with these vectors.

We next wanted to compare the I_{SA} currents recorded in identified CA1 pyramidal neurons in slice culture with those from pyramidal neurons recorded in dissociated culture to compare the channel densities, basic gating properties and importance of Kv4 channels for this current. No significant differences were noted in steady-state gating properties or kinetics of I_{SA} currents in these two systems. Peak conductance density for I_{SA} recorded in dissociated cultured hippocampal pyramidal neurons or CA1 pyramidal neurons in organotypic culture were also not significantly different, and averaged around 950 pS/pF, see Fig. 10(a). Given an estimated conductance for I_{SA} channels of 6 pS, this corresponds to

roughly 1.5–1.7 channels per square micron open at the peak conductance under both conditions (Chen and Johnston 2004).

We next examined the specific effects of these viral vectors on the I_{SA} currents in infected CA1 neurons in organotypic culture. In agreement with our studies in dissociated culture, expression of Kv4DN-EGFP and Kv4.2 in CA1 pyramidal neurons selectively suppresses the levels of I_{SA} current without affecting other voltage-gated potassium currents. Kv4DN-EGFP suppressed I_{SA} by 60%, an amount similar to what we had previously seen in dissociated neuronal culture (Fig. 10b). Increasing transcription of Kv4.2 in CA1 pyramidal neurons increases the levels of I_{SA} current to 175% of its original level, similar to what we have seen in dissociated cultures (Fig. 10d). Comparison of these data across groups shows that there are no significant differences in the effects on I_{SA} current amplitude between expression of Kv4DN-EGFP in dissociated neuronal culture and CA1 neurons in organotypic slice culture (Fig. 10c). Likewise, the amplitude increase produced by over-expression of Kv4.2 is not significantly different between these two systems (Fig. 10e). We further compared the biophysical properties between these I_{SA} currents recorded under these various conditions and we did not observe any significant differences in I_{SA} channel function. We therefore conclude that I_{SA} currents in hippocampal pyramidal neuron recorded in dissociated culture under our conditions largely reflect the current density and regulatory properties of CA1 neurons in hippocampal neuron in organotypic slice culture.

Discussion

Using a novel approach combining careful biophysical separation of currents with RNA interference and over-expression, we have identified Kv4.2 (KCND2) as a critical gene in the formation and regulation of I_{SA} current amplitude in hippocampal pyramidal neurons. Our studies in hippocampal pyramidal neurons in dissociated culture and CA1 pyramidal neurons in organotypic culture have shown that a distinct A-current component, the I_{SA} current, is tightly regulated by changes in Kv4.2 channel transcription. Suppression of Kv4.2 expression using RNAi suppresses I_{SA}, whereas increasing the level of Kv4.2 transcripts increases the amplitude of I_{SA}. These studies therefore clearly identify Kv4.2 as a critical gene in the formation of hippocampal pyramidal I_{SA} current. Our results also suggest a likely dynamic aspect to this regulation, with a role for the Kv4.2 gene in regulating the I_{SA} current amplitude through changes in gene transcription. Previous *in situ* hybridization and immunohistochemistry studies have shown that the Kv4.2 gene is highly expressed in hippocampal pyramidal neurons; therefore, our studies directly link these specific gene products, present in these neurons, to the selective formation of the I_{SA} component of A-current (Serodio *et al.* 1996; Rhodes *et al.* 2004).

The I_{SA} current in cultured hippocampal pyramidal neurons formed from Kv4.2 subunits has a half activation potential of −22.1 ± 2.9 mV and a half inactivation potential of −70.1 ± 2.2 mV. This very negative half inactivation potential is considerably more hyperpolarized than the typical resting potential we record in these neurons, around −61 ± 2.9 mV. From our steady-state inactivation curve for I_{SA} (Fig. 2a), this means that more than two-thirds of the I_{SA} channels in these neurons are typically inactivated at rest. In contrast, the I_{AD} current has a half inactivation potential of −11.4 ± 2.3 mV (Fig. 2b), and therefore is likely not inactivated at all at rest. The activation of the I_{AD} current with a midpoint of +28.9 ± 3.3 mV requires much larger depolarizations than I_{SA}. Therefore, it is clear that in native neurons the molecular compositions and functional ranges of these two A-type channel types are distinct.

Although Kv4.2 RNA interference selectively suppresses 60% of the I_{SA} at 48 h, the identity of the residual unsuppressed I_{SA} current component is unclear. Biophysical characterization

of this residual I_{SA} current suggests that the channels composing this current are very similar to the Kv4.2-sensitive current, making it likely that Kv4 family members are responsible for this current. In addition to Kv4.2, Kv4.3 is also expressed in the hippocampus, although at higher levels in interneurons, therefore it may be responsible for this residual current component (Rhodes *et al.* 2004). Interestingly, dominant-negative constructs that suppress all Kv4 channels suppress the I_{SA} current to a similar extent as Kv4.2 RNA interference. Although neither RNA interference nor dominant-negative constructs are expected to suppress current by 100%, the simplest explanation for this common result is Kv4.2 is required for all I_{SA} current expression and that 40% unsuppressed I_{SA} current reflects channels that are not turned over in 48 h. If this is so, then Kv4.3 may not efficiently form I_{SA} channels on it own in pyramidal neurons, similar to the heart where a Kv4.2 knockout mouse was shown to lack $I_{to,f}$ despite the fact that Kv4.3 expression still remains, suggesting that Kv4.2 has a special role in the surface expression of function $I_{to,f}$ channels (Guo *et al.* 2005). However, we must consider the fact that the apparent similarity in the effects of RNA interference and dominant-negative constructs may be a fortuitous result. In our future studies, we will examine the time course of Kv4.2 protein turnover in neurons, and removal from the cell surface, to determine if the 40% residual current is a result of either the slow turnover of all channels, or the presence of a more stable fraction of channels that turns over slowly. In addition, we are developing lentiviral vectors that should allow us to examine the currents in infected neurons expressing Kv4.2-RNAi or Kv4DN-EGFP at longer time points, as well as vectors that can suppress Kv4.3 to determine the exact molecular composition of this residual I_{SA} current.

Our studies also reveal several important aspects of I_{SA} current regulation that will require further study to fully understand the underlying mechanisms. The first is that the amplitude of I_{SA} is similar in hippocampal pyramidal neurons recorded in either dissociated culture or organotypic culture, at approximately 1000 pS/pF of current. It is therefore possible that, despite the significant differences in circuitry in these two culture systems, major aspects of the intrinsic genetic program that is regulating I_{SA} are conserved. Future studies will be required to determine what factors are acting in these systems to regulate I_{SA} current around this apparent set point.

A second interesting observation is that increases in I_{SA} amplitude produced by over-expression of Kv4.2 are limited to around 170% of the normal current level regardless of vector system being used or whether the experiments were in dissociated or organotypic cultures. A further surprise is that this enhanced I_{SA} current is indistinguishable from the normal I_{SA} current. If Kv4.2 is expressed alone in the heterologous system, the biophysical properties of the expressed channels are quite distinct from native I_{SA} (Jerng *et al.* 2005). Expressed alone, Kv4.2 inactivation occurs with three exponential kinetic components and recovery from inactivation requires hundreds of milliseconds. In addition, the kinetics of Kv4.2 inactivation become more rapid with depolarization, not slower as seen with native I_{SA}. Only when Kv4.2 is co-expressed with KChIP and DPL auxiliary proteins do the functional properties of channels expressed in heterologous cells become similar to native I_{SA} channels in kinetics and voltage-dependence (Jerng *et al.* 2004b, 2005). KChIP binding removes an N-type inactivation mechanism from the channel, the most of the channel inactivation to occur through a single closed-state mechanism that becomes slower with depolarization (Bahring *et al.* 2001; Gebauer *et al.* 2004; Zhou *et al.* 2004). DPL binding accelerates the kinetics of Kv4.2 channel gating to the rates similar to what is seen with native channels (Nadal *et al.* 2003; Jerng *et al.* 2005). Thus, we suggest that an intrinsic regulatory mechanism is acting in neurons to limit the surface expression of Kv4.2 subunits if they lack auxiliary subunit proteins.

Studies in heterologous systems show that Kv4.2 protein surface expression is strongly dependent on the presence of auxiliary subunits, with a 12–40-fold increase in current expression when Kv4.2 is co-expressed with KChIP and DPL auxiliary subunits (An *et al.* 2000; Bahring *et al.* 2001; Nadal *et al.* 2003; Jerng *et al.* 2004a; Zhou *et al.* 2004; Jerng *et al.* 2005). If similar effects are occurring in native neurons, then Kv4.2 channels that do not co-assemble with auxiliary subunits would only be put onto the cell surface with an efficiency 2.5% of those with auxiliary subunits. This low efficiency would effectively clamp the maximum level for over-expression of I_{SA} to a point limited by the native availability of KChIP and DPL subunits in these neurons. Thus, a possible hypothesis to explain these results is that native KChIP and DPL expression levels are slightly higher than Kv4.2, sufficient for 70% more channels than are provided by native Kv4.2 subunit expression. An alternative possible explanation is that auxiliary proteins are not limiting at all, but native feedback mechanisms act to limit the amount of the protein increase onto the cell surface. Future studies will attempt to distinguish between these hypotheses by targeting auxiliary subunits with RNA interference, and over-expressing auxiliary subunits with or without Kv4.2 to determine a possible role for auxiliary protein expression in limiting the maximum surface density for I_{SA} channels.

Acknowledgments

We would like to thank Dr David Johns for the Kv4 Dominant-negative mutant EGFP-tagged construct and Dr Daniel Johnston for his advice and support. This work was supported by NIH Grants NS37444 and MH48432 and NS31583.

Abbreviations used

CMV	Cytomegalovirus IE promoter
DPL	Dipeptidyl peptidase like protein
EGFP	enhanced green fluorescent protein
ER	endoplasmic reticulum
GADPH	glyceraldehyde 3-phosphate dehydrogenase
HpTx3	heteropodatoxin-3
KChIP	Kv channel interacting proteins
MEM	minimal essential medium
PB	phosphate buffer
RNAi	RNA interference
UT	uninfected neuron terminals

References

An WF, Bowlby MR, Betty M, et al. Modulation of A-type potassium channels by a family of calcium sensors. Nature. 2000; 403:553–556. [PubMed: 10676964]

Bahring R, Dannenberg J, Peters HC, Leicher T, Pongs O, Isbrandt D. Conserved Kv4 N-terminal domain critical for effects of Kv channel-interacting protein 2.2 on channel expression and gating. J. Biol. Chem. 2001; 276:23 888–23 894.

Baldwin TJ, Tsaur ML, Lopez GA, Jan YN, Jan LY. Characterization of a mammalian cDNA for an inactivating voltage-sensitive K^+ channel. Neuron. 1991; 7:471–483. [PubMed: 1840649]

Barry DM, Xu H, Schuessler RB, Nerbonne JM. Functional knockout of the transient outward current, long-QT syndrome, and cardiac remodeling in mice expressing a dominant-negative Kv4α subunit. Circ. Res. 1998; 83:560–567. [PubMed: 9734479]

Bernard C, Legros C, Ferrat G, Bischoff U, Marquardt A, Pongs O, Darbon H. Solution structure of hpTX2, a toxin from *Heteropoda venatoria* spider that blocks Kv4.2 potassium channel. Protein Sci. 2000; 9:2059–2067. [PubMed: 11152117]

Brummelkamp TR, Bernards R, Agami R. A system for stable expression of short interfering RNAs in mammalian cells. Science. 2002; 296:550–553. [PubMed: 11910072]

Cai X, Liang CW, Muralidharan S, Kao JP, Tang CM, Thompson SM. Unique roles of SK and Kv4.2 potassium channels in dendritic integration. Neuron. 2004; 44:351–364. [PubMed: 15473972]

Chen X, Johnston D. Properties of single voltage-dependent K^+ channels in dendrites of CA1 pyramidal neurones of rat hippocampus. J. Physiol. 2004; 559:187–203. [PubMed: 15218076]

Couzin J. Breakthrough of the year. Small RNAs make big splash. Science. 2002; 298:2296–2297. [PubMed: 12493875]

Frick A, Magee J, Johnston D. LTP is accompanied by an enhanced local excitability of pyramidal neuron dendrites. Nat. Neurosci. 2004; 7:126–135. [PubMed: 14730307]

Gebauer M, Isbrandt D, Sauter K, Callsen B, Nolting A, Pongs O, Bahring R. N-type inactivation features of Kv4.2 channel gating. Biophys. J. 2004; 86:210–223. [PubMed: 14695263]

Gu N, Vervaeke K, Hu H, Storm JF. Kv7/KCNQ/M and HCN/h, but not KCa2/SK channels, contribute to the somatic medium after-hyperpolarization and excitability control in CA1 hippocampal pyramidal cells. J. Physiol. 2005; 566:689–715. [PubMed: 15890705]

Guo W, Jung WE, Marionneau C, Aimond F, Xu H, Yamada KA, Schwarz TL, Demolombe S, Nerbonne JM. Targeted deletion of Kv4.2 eliminates $I_{to,f}$ and results in electrical and molecular remodeling, with no evidence of ventricular hypertrophy or myocardial dysfunction. Circ. Res. 2005; 97:1342–1350. [PubMed: 16293790]

Hoffman DA, Magee JC, Colbert CM, Johnston D. K^+ channel regulation of signal propagation in dendrites of hippocampal pyramidal neurons. Nature. 1997; 387:869–875. [PubMed: 9202119]

Jan LY, Jan YN. Cloned potassium channels from eukaryotes and prokaryotes. Annu. Rev. Neurosci. 1997; 20:91–123. [PubMed: 9056709]

Jasinska R, Zhang QX, Pilquil C, et al. Lipid phosphate phosphohydrolase-1 degrades exogenous glycerolipid and sphingolipid phosphate esters. Biochem. J. 1999; 340:677–686. [PubMed: 10359651]

Jerng HH, Qian Y, Pfaffinger PJ. Modulation of Kv4.2 channel expression and gating by dipeptidyl peptidase 10 (DPP10). Biophys. J. 2004a; 87:2380–2396. [PubMed: 15454437]

Jerng HH, Pfaffinger PJ, Covarrubias M. Molecular physiology and modulation of somatodendritic A-type potassium channels. Mol. Cell Neurosci. 2004b; 27:343–369. [PubMed: 15555915]

Jerng HH, Kunjilwar K, Pfaffinger PJ. Multiprotein assembly of Kv4.2, KChIP3 and DPP10 produces ternary channel complexes with ISA-like properties. J. Physiol. 2005; 568:767–788. [PubMed: 16123112]

Jeromin A, Yuan LL, Frick A, Pfaffinger P, Johnston D. A modified Sindbis vector for prolonged gene expression in neurons. J. Neurophysiol. 2003; 90:2741–2745. [PubMed: 12853440]

Johns DC, Nuss HB, Marban E. Suppression of neuronal and cardiac transient outward currents by viral gene transfer of dominant-negative Kv4.2 constructs. J. Biol. Chem. 1997; 272:31 598–31 603.

Johnston D, Christie BR, Frick A, Gray R, Hoffman DA, Schexnayder LK, Watanabe S, Yuan LL. Active dendrites, potassium channels and synaptic plasticity. Philos. Trans. R. Soc. Lond. B Biol. Sci. 2003; 358:667–674. [PubMed: 12740112]

Kim J, Wei DS, Hoffman DA. Kv4 potassium channel subunits control action potential repolarization and frequency dependent broadening in hippocampal CA1 pyramidal neurons. J. Physiol. 2005; 569:41–57. [PubMed: 16141270]

Malgaroli A, Tsien RW. Glutamate-induced long-term potentiation of the frequency of miniature synaptic currents in cultured hippocampal neurons. Nature. 1992; 357:134–139. [PubMed: 1349728]

McCabe JB, Berthiaume LG. Functional roles for fatty acylated amino-terminal domains in subcellular localization. Mol. Biol. Cell. 1999; 10:3771–3786. [PubMed: 10564270]

Misonou H, Mohapatra DP, Trimmer JS. Kv2.1: a voltage-gated K^+ channel critical to dynamic control of neuronal excitability. Neurotoxicology. 2005; 26:743–752. [PubMed: 15950285]

Mu J, Zhuang SY, Kirby MT, Hampson RE, Deadwyler SA. Cannabinoid receptors differentially modulate potassium A and D currents in hippocampal neurons in culture. J. Pharmacol. Exp. Ther. 1999; 291:893–902. [PubMed: 10525114]

Nadal MS, Ozaita A, Amarillo Y, et al. The CD26-related dipeptidyl aminopeptidase-like protein DPPX is a critical component of neuronal A-type K^+ channels. Neuron. 2003; 37:449–461. [PubMed: 12575952]

Ramakers GM, Storm JF. A postsynaptic transient K^+ current modulated by arachidonic acid regulates synaptic integration and threshold for LTP induction in hippocampal pyramidal cells. Proc. Natl Acad. Sci. USA. 2002; 99:10 144–10 149. [PubMed: 11782544]

Reynolds ES. The use of lead citrate at high pH as an electron-opaque stain in electron microscopy. J. Cell Biol. 1963; 17:208–212. [PubMed: 13986422]

Rhodes KJ, Carroll KI, Sung MA, et al. KChIPs and Kv4a subunits as integral components of A-type potassium channels in mammalian brain. J. Neurosci. 2004; 24:7903–7915. [PubMed: 15356203]

Sanguinetti MC, Johnson JH, Hammerland LG, Kelbaugh PR, Volkmann RA, Saccomano NA, Mueller AL. Heteropodatoxins: peptides isolated from spider venom that block Kv4.2 potassium channels. Mol. Pharmacol. 1997; 51:491–498. [PubMed: 9058605]

Schrader LA, Anderson AE, Varga AW, Levy M, Sweatt JD. The other half of Hebb: K^+ channels and the regulation of neuronal excitability in the hippocampus. Mol. Neurobiol. 2002; 25:51–66. [PubMed: 11890457]

Serodio P, Vega-Saenz de Miera E, Rudy B. Cloning of a novel component of A-type K^+ channels operating at subthreshold potentials with unique expression in heart and brain. J. Neurophysiol. 1996; 75:2174–2179. [PubMed: 8734615]

Sheng M, Tsaur ML, Jan YN, Jan LY. Subcellular segregation of two A-type K^+ channel proteins in rat central neurons. Neuron. 1992; 9:271–284. [PubMed: 1497894]

Song WJ, Tkatch T, Baranauskas G, Ichinohe N, Kitai ST, Surmeier DJ. Somatodendritic depolarization-activated potassium currents in rat neostriatal cholinergic interneurons are predominantly of the A type and attributable to co-expression of Kv4.2 and Kv4.1 subunits. J. Neurosci. 1998; 18:3124–3137. [PubMed: 9547221]

Stoppini L, Buchs PA, Muller D. A simple method for organotypic cultures of nervous tissue. J. Neurosci. Meth. 1991; 37:173–182.

Surmeier DJ, Bargas J, Kitai ST. Two types of A-current differing in voltage-dependence are expressed by neurons of the rat neostriatum. Neurosci. Lett. 1989; 103:331–337. [PubMed: 2812520]

Tkatch T, Baranauskas G, Surmeier DJ. Kv4.2 mRNA abundance and A-type K^+ current amplitude are linearly related in basal ganglia and basal forebrain neurons. J. Neurosci. 2000; 20:579–588. [PubMed: 10632587]

Watanabe S, Hoffman DA, Migliore M, Johnston D. Dendritic K^+ channels contribute to spike-timing dependent long-term potentiation in hippocampal pyramidal neurons. Proc. Natl Acad. Sci. USA. 2002; 99:8366–8371. [PubMed: 12048251]

Wickenden AD, Lee P, Sah R, Huang Q, Fishman GI, Backx PH. Targeted expression of a dominant-negative K(v)4.2 K(+) channel subunit in the mouse heart. Circ. Res. 1999; 85:1067–1076. [PubMed: 10571538]

Wu RL, Barish ME. Two pharmacologically and kinetically distinct transient potassium currents in cultured embryonic mouse hippocampal neurons. J. Neurosci. 1992; 12:2235–2246. [PubMed: 1607938]

Yuan LL, Adams JP, Swank M, Sweatt JD, Johnston D. Protein kinase modulation of dendritic K^+ channels in hippocampus involves a mitogen-activated protein kinase pathway. J. Neurosci. 2002; 22:4860–4868. [PubMed: 12077183]

Zarayskiy VV, Balasubramanian G, Bondarenko VE, Morales MJ. Heteropoda toxin 2 is a gating modifier toxin specific for voltage-gated K^+ channels of the Kv4 family. Toxicon. 2005; 45:431–442. [PubMed: 15733564]

Zhou W, Qian Y, Kunjilwar K, Pfaffinger PJ, Choe S. Structural insights into the functional interaction of KChIP1 with Shal-type K^+ channels. Neuron. 2004; 41:573–586. [PubMed: 14980206]

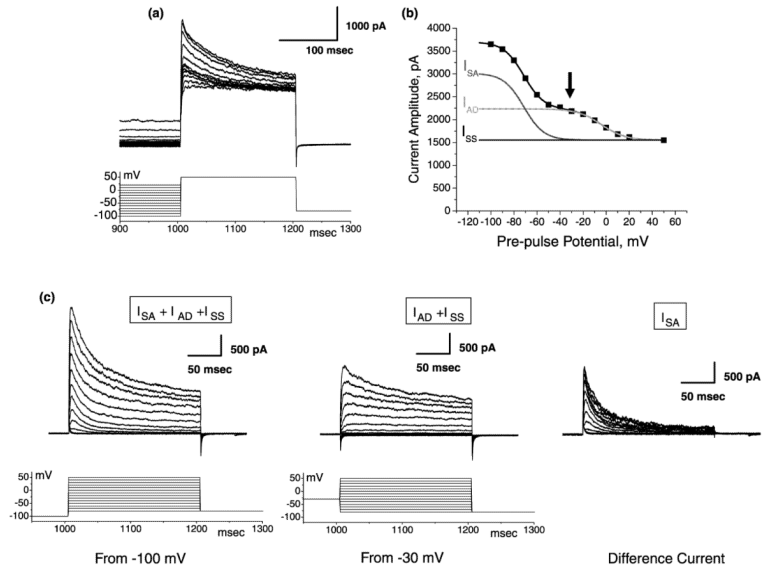

Fig. 1.

Differential inactivation properties allow the separation of I_{SA} from other voltage-gated potassium currents. (a) Inactivation of native Kv channels in response to pre-pulse potentials applied for 1 s from −100 to +20 mV in 10-mV steps. Currents are elicited by a test pulse to +50 mV. Current traces bunch together in a middle voltage range from −50 to −30 mV (b) Native Kv currents separate into two clear components of inactivating current, I_{SA} and I_{AD}, and a sustained component, I_{SS}. Voltage pre-pulses between −30 and −40 mV selectively suppress I_{SA} without inactivating I_{AD}. (c) Difference currents measured between recordings from holding potentials of −100 mV and −30 mV isolate the I_{SA} current.

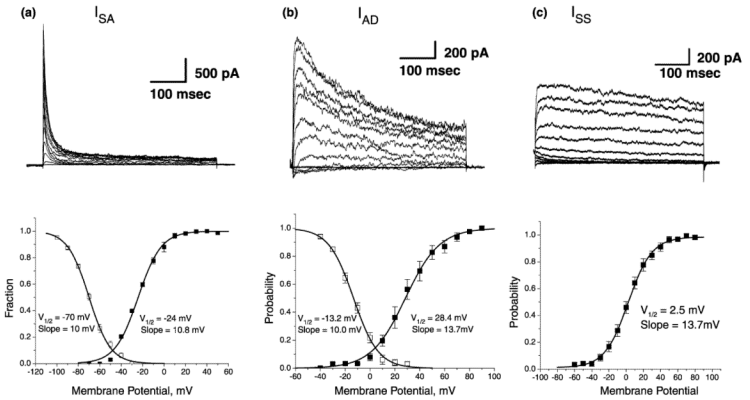

Fig. 2.

Activation and inactivation properties of characterized voltage-gated potassium currents. (a) Isolated I_{SA} current traces in response to 500-ms depolarizations from −70 to +50 mV. I_{SA} isolated as a difference current between recordings obtained with a 500-ms pre-pulse to −100 mV versus a pre-pulse to −30 mV. Inactivation of isolated I_{SA} is very rapid and nearly complete in the first 50 ms. Peak activation and steady-state inactivation curves for isolated I_{SA} current. (b) Isolated I_{AD} current traces in response to 500-ms depolarizations from −60 to +80 mV. I_{AD} was isolated from I_{SS} by subtraction of traces obtained with a 500-ms pre-pulse to +50 mV from traces recorded from a holding potential of −30 mV. The accuracy of the subtraction was improved by stepping the +50-mV traces back to −30 mV for 15 ms before the test pulse was applied to provide enough time for most of the I_{SS} channels to close, but not allow the I_{AD} channels to recover from inactivation. Following isolation, it is clear that I_{AD} inactivation is slower than I_{SA}, as evident by comparison with traces in (a). Peak activation and steady-state inactivation curves for isolated I_{AD} current. (c) Isolated I_{SS} current traces in response to 500-ms depolarization from −60 to +80 mV. I_{SS} isolated by pulsing to +50 mV for 500 ms, to inactivate I_{AD}, then shutting the I_{SS} channels with a 10-ms pulse to −30 mV before re-opening by a test pulse. Peak activation curve for isolated I_{SS} current.

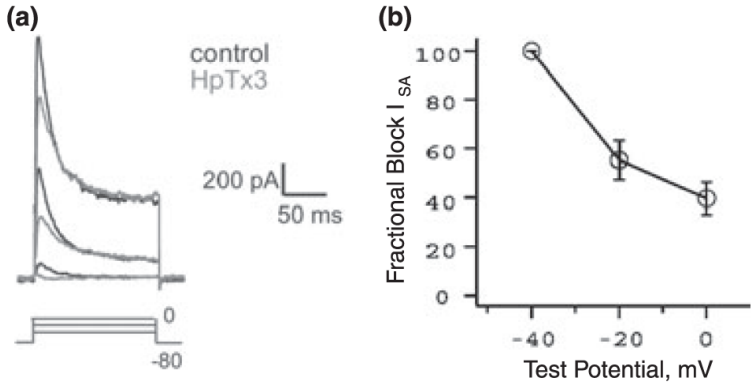

Fig. 3.

HpTx3 selectively suppresses I_{SA} in a voltage-dependent manner. (a) Total outward current in cultured hippocampal pyramidal neuron before and after application of 100 n_M HpTx3. Selective suppression of the rapidly inactivating I_{SA} current is evident by the restricted effect of the toxin during the first 50 ms of the depolarization before I_{SA} inactivates, see Fig. 2(a and b). Fractional loss of I_{SA} is highly voltage dependent ($n = 3$).

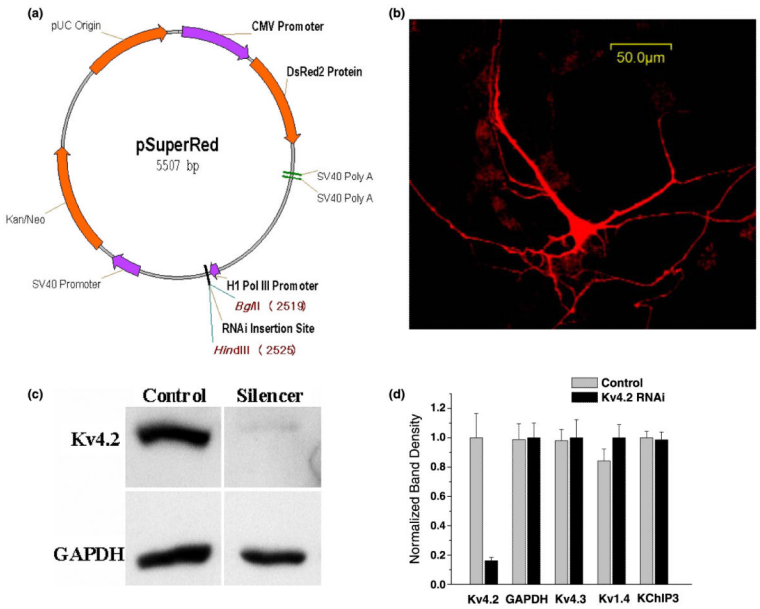

Fig. 4.

pSuperRed-Kv4.2i selectively suppresses the expression of Kv4.2. (a) pSuperRed expressed DsRed2 from a CMV promoter and shRNAs from the H1 Pol III promoter. ShRNA sequences are directionally inserted into the *Bgl*II-*Hind*III sites. (b) pSuperRed clearly marks transfected pyramidal neurons in culture which are expressing interfering RNAs. (c) pSuperRed-Kv4.2i strongly suppresses the expression of Kv4.2 in COS7 cells. (d) Summary data shows that pSuperRed-Kv4.2i selectively suppresses Kv4.2 and not other potential A-current subunits. Control pSuperRed has no effect on expression of any subunit (each condition is an average of nine separate transfections).

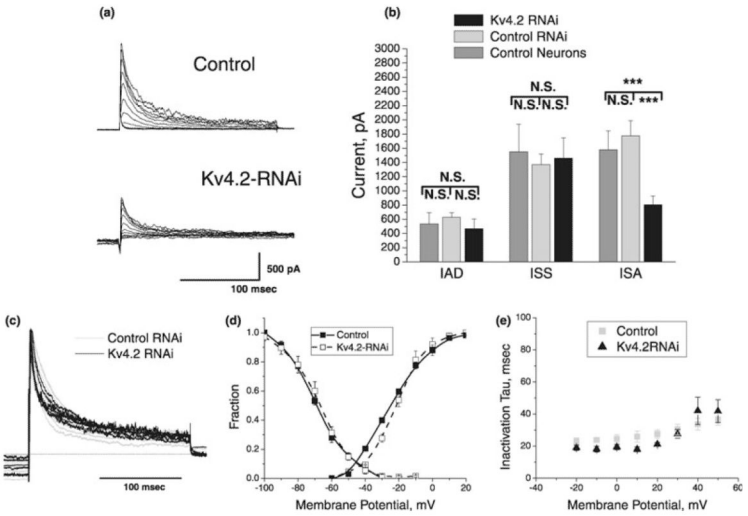

Fig. 5.

Kv4.2 RNA interference selectively suppresses I_{SA}. (a) Representative I_{SA} current traces from neuron expressing pSuperRed (Control) or pSuperRed-Kv4.2i (Kv4.2-RNAi). I_{SA} component of current was recorded as described in Fig. 1(c). (b) Summary data shows Kv4.2-RNAi selectively suppresses the I_{SA} component of voltage-gated potassium current and has no significant effect on I_{AD} or I_{SS} (untransfected, $n = 9$; pSuperRed, $n = 12$; pSuperRed-Kv4.2i, $n = 7$). (c) I_{SA} currents in response to a pulse to +50 mV are scaled by normalized to peak current during the pulse and overlapped from control and Kv4.2-RNAi expressing neurons. The shape of the I_{SA} current during the pulse to +50 mV is similar in both conditions, showing that the residual I_{SA} current is kinetically similar to the total I_{SA} current. The variable baseline level in the pre-pulse current is a subtraction artifact, as described in Materials and methods, that does not affect the test or tail pulse currents. (d) I_{SA} current activation and inactivation curves for recordings from control and Kv4.2-RNAi expressing neurons. (e) Voltage-dependence for inactivation time constant for the I_{SA} current in control and Kv4.2-RNAi expressing neurons (pSuperRed, $n = 9$; pSuperRed-Kv4.2i, $n = 4$). Both show a similar range of time constants and slowing of inactivation with depolarization.

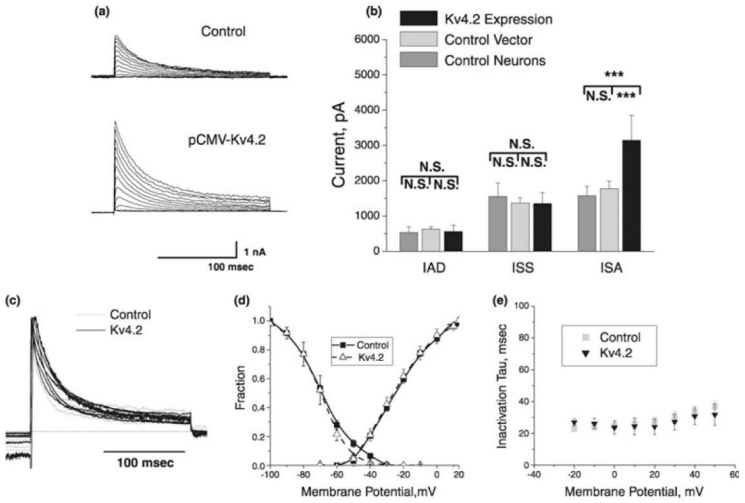

Fig. 6.

Increasing the expression of Kv4.2 selectively increases I_{SA}. (a) Representative I_{SA} current traces from neuron expressing empty pSuperRed (Control) or pCMV-Kv4.2. I_{SA} component of current was recorded as described in Fig. 1(c). (b) Summary data shows Kv4.2 expression selectively increases the I_{SA} component of voltage-gated potassium current and has no significant effect on I_{AD} or I_{SS}. (un-transfected, $n = 9$; pSuperRed, $n = 12$; pCMV-Kv4.2, $n = 8$). (c) I_{SA} currents in response to a pulse to +50 mV are normalized to peak current during the pulse and overlapped from control and Kv4.2-expressing neurons. The shape of the I_{SA} current during the pulse to +50 mV is similar in both conditions, showing that over-expressed I_{SA} current is kinetically similar to the native I_{SA} current. The variable baseline level in the pre-pulse current is a subtraction artifact, as described in Materials and methods, that does not affect the test or tail pulse currents. (d) I_{SA} current activation and inactivation curves for recordings from control and Kv4.2-expressing neurons. (e) Voltage-dependence for inactivation time constant for the I_{SA} current in control and Kv4.2-expressing neurons (pSuperRed, $n = 9$; pCMV-Kv4.2, $n = 4$). Both show a similar range of time constants and slowing of inactivation with depolarization.

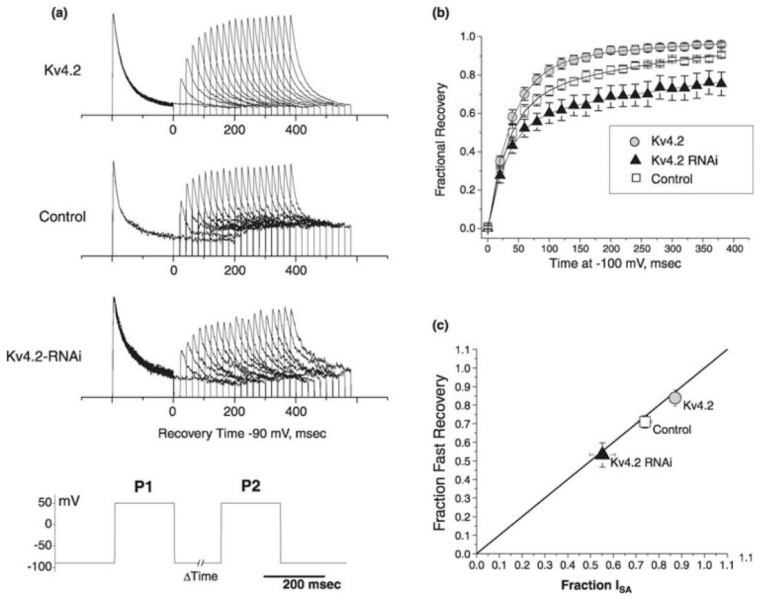

Fig. 7.

Modulating I_{SA} amplitude selectively modulates the amplitude of the fast component for recovery from inactivation. (a) Representative traces during recovery from inactivation for neurons transfected with Kv4.2, pSuperRed (control) or pSuperRed-Kv4.2i measured using two pulse protocols with a variable interpulse time at −90 mV. Currents are scaled to the same size. (b) Recovery from inactivation shows a two-exponential time course for all three types of neurons [average values of τ_f = 34.1 ± 2.4 ms and τ_s = 542 ± 123 ms, with no significant differences in taus among the different groups (n = 16)]. The relative size of the fast component to the slow component is increased with Kv4.2 expression and decreased with Kv4.2-RNAi, as expected if this component is because of I_{SA} (pSuperRed-Kv4.2i, n = 7; pSuperRed, n = 7; pCMV-Kv4.2, n = 4). (c) Comparison of the fraction of total A-current that is because of I_{SA}: Fraction I_{SA} = (I_{SA}/ (I_{SA} + I_{AD}) (see Figs 5b and 6b) to the fraction of the total recovery from inactivation that occurs with a fast kinetic: Fraction Fast Recovery = (A_f/(A_f + A_s) (see Fig. 7b). The data vary along the identity line as expected if the fast recovery component is because of I_{SA} and the slow recovery component is as a result of I_{AD}.

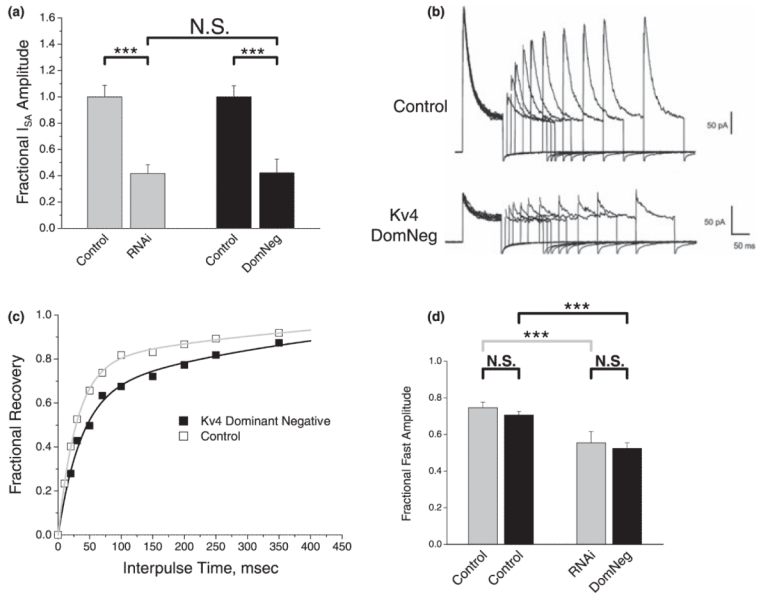

Fig. 8.

Expression of a dominant-negative Kv4 construct suppresses I_{SA} to a similar extent as Kv4.2 RNA interference. (a) Summary graph comparing the suppression of I_{SA} by Kv4.2-RNAi ($n = 7$) with the suppression by Kv4DN-EGFP ($n = 8$). Both approaches suppress current to the same extent. (b) Inactivation recovery traces for control neurons transfected with EGFP compared with Kv4DN-EGFP, recorded in outside-out patches. The currents are significantly smaller with Kv4DN-EGFP and recover more slowly. (c) Fits to normalized recovery data show the two exponential components of total A-current recovery. Amplitude of the fast component decreases with Kv4DN-EGFP expression. (d) Summary data comparing the change in the amplitude of the fast recovery time constant following Kv4.2-RNAi ($n = 7$) or Kv4DN-EGFP ($n = 3$) expression. Both suppress the fast component of recovery to a similar extent.

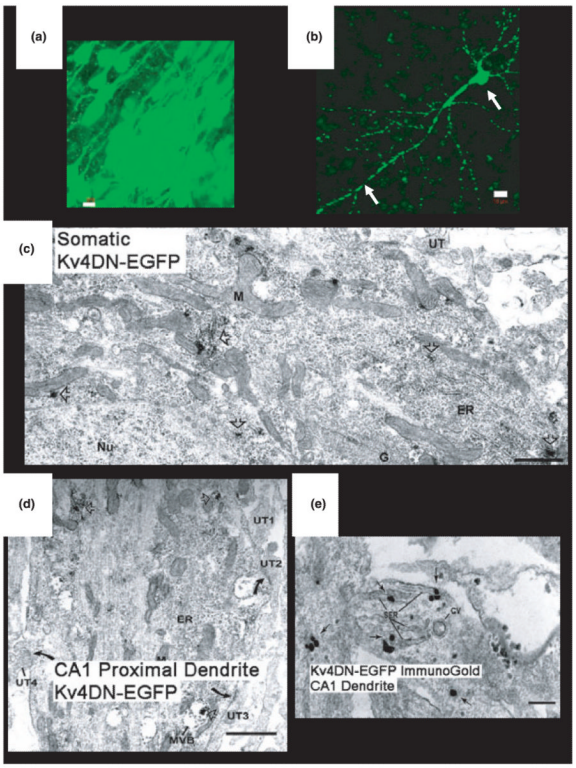

Fig. 9.

Sindbis vectors express Kv4.2 and Kv4 dominant-negative constructs in CA1 pyramidal neurons in organotypic culture. (a) High-powered view of CA1 pyramidal neurons infected with Sindbis-Kv4.2 that co-expresses EGFP. Entire cell fills evenly with green fluorescence. Scale bar = 5 μm. (b) Single CA1 pyramidal neuron infected with Sindbis-Kv4DN-EGFP. In these cells there is an uneven distribution of green fluorescence that is restricted to the somatodendritic compartments. Labeling hot spots are indicated. Scale bar = 10 μm. (c) Electron micrograph from the hippocampal CA1 region showing a neuronal perikaryon from a pyramidal neuron infected with Sindbis-Kv4DN-EGFP. Immunoperoxidase labeling for Kv4DN-EGFP (open arrows) is seen as a black precipitate distributed mainly along the ER membrane. The labeled soma is receiving a synaptic input from an unlabeled terminal (UT). G, Golgi stacks; M, mitochondri; Nu, nucleus. Scale bar = 1 μm. (d) Electron micrograph from CA1 pyramidal neuron proximal dendrite of neuron infected with Kv4DN-EGFP. Immunoperoxidase labeling (open arrows) is diffusely distributed within the cytoplasm and appears to be most prevalent along membranes of the ER as well as on elements of the cytoskeleton. Immunoperoxidase labeling is also evident within a multivesicular body (MVB). The dendrite receives multiple asymmetric (curved arrow) synapses from unlabeled terminals (UT2-4) that show no immunoperoxidase label. M, mitochondrion. Scale bar = 1 μm. (e) Subcellular distribution for Kv4DN-EGFP in dendrites quantitated by immunogold labeling. Gold particles are found primarily in the cytoplasm and are most prevalent along the membranes of the smooth endoplasmic reticulum (SER; arrows). Note a coated vesicle (CV) near the SER. Scale bars = 0.2 μm.

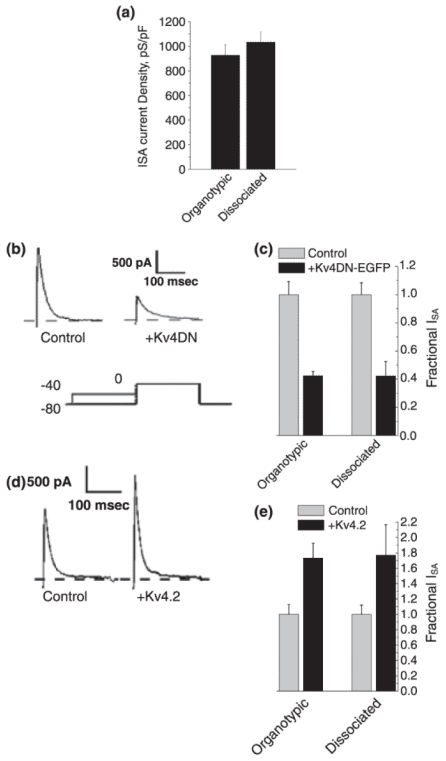

Fig. 10.

Regulation of I_{SA} expression is similar in dissociated hippocampal pyramidal neurons and CA1 pyramidal neurons in organotypic culture. (a) Peak conductance density for I_{SA} in dissociated hippocampal pyramidal neurons ($n = 9$) and organotypic CA1 pyramidal neurons ($n = 7$) are not significantly different. (b) Sindbis-Kv4DN-EGFP suppresses I_{SA} current amplitude in CA1 pyramidal neurons in organotypic culture. Representative I_{SA} currents obtained from these studies are shown as different currents obtained by subtracting a depolarization to 0 mV with a pre-pulse to −40 mV from a matched recording with a pre-pulse to −80 mV. (c) Summary data show that suppression of I_{SA} by Kv4DN-EGFP is similar in organotypic dissociated culture ($n = 9$) to suppression seen in dissociated culture ($n = 8$). (d) Increasing expression of Kv4.2 in CA1 pyramidal neurons by Sindbis-Kv4.2 increases the amplitude of I_{SA}. I_{SA} was isolated as described in (b). (e) Summary data shows that the increase in current is similar for pCMV-Kv4.2 expression in dissociated pyramidal neurons ($n = 8$) and Sindbis-Kv4.2 infection of CA1 pyramidal neurons in organotypic culture ($n = 5$).